

Supplementary Information for

A universal synthesis strategy to make metal nitride electrocatalysts for hydrogen evolution reaction

Luo Yu^{1,2}, Shaowei Song², Brian McElhenny², Fazhu Ding^{2,3}, Dan Luo², Ying Yu^{1,*}, Shuo Chen^{2,*},
and Zhifeng Ren^{2,*}

¹ College of Physical Science and Technology, Central China Normal University, Wuhan 430079, China

² Department of Physics and TcSUH, University of Houston, Houston, TX 77204, USA

³ Key Laboratory of Applied Superconductivity and Institute of Electrical Engineering, Chinese Academy of Sciences, Beijing 100190, China

* Corresponding author. Email: yuying01@mail.ccnu.edu.cn (Y.Y); schen34@uh.edu (S. C.); and zren@uh.edu (Z. F. R.).

1. Experimental Section

Chemicals. Hydrochloric acid (HCl, AR, MACRON), ethanol (C₂H₅OH, Decon Labs, Inc.), nickel (II) nitrate hexahydrate [Ni(NO₃)₂·6H₂O, 98%, Sigma-Aldrich], cobalt (II) nitrate hexahydrate [Co(NO₃)₂·6H₂O, 98%, Sigma-Aldrich], iron (III) nitrate hexahydrate [Fe(NO₃)₃·9H₂O, 98%, Sigma-Aldrich], N, N Dimethylformamide [DMF, (CH₃)₂NC(O)H, anhydrous, 99.8%, Sigma-Aldrich], platinum powder (Pt, nominally 20% on carbon black, Alfa Aesar), Nafion (117 solution, 5% wt, Aldrich), potassium hydroxide (KOH, 50% w/v, Alfa Aesar), and Ni foam (thickness: 1.6 mm) were used as received. Deionized water (resistivity: 18.3 MΩ·cm) was used for the preparation of all aqueous solutions.

Synthesis of metal nitrides on different substrates. For the synthesis of the monometallic nitrides, the Co, Fe, and Ni precursor inks were prepared by dissolving Co(NO₃)₂·6H₂O, Ni(NO₃)₂·6H₂O, and Fe(NO₃)₃·9H₂O in DMF, respectively, and Ni foam was soaked in the different precursor inks and dried at ambient conditions. Thermal nitridation then conducted on the dried samples at 500 °C in a tube furnace under a flow of 120 standard cubic centimeters (sccm) of NH₃ and 30 sccm Ar for 1 h. The samples were labeled CoN, Fe₄N, and Ni₃N, respectively. The samples of CoN on Cu foam, carbon paper, and stainless-steel mat were synthesized using the same procedure, only changing the substrate. The bimetallic nitrides on the Ni foam were also synthesized using the same method, only mixing the precursor inks of Ni and Fe, Co and Fe, Ni and Co, each with a mole ratio of 1:1. The three samples were labeled NiFeN, CoFeN, and NiCoN, respectively. To synthesize different compositions of Ni-doped CoN on the Ni foam, we changed the respective concentrations of the Ni and Co inks. The samples were labeled Ni₂CoN, NiCoN, NiCo₂N, and NiCo₃N according to the mole ratio of Ni and Co in the precursors.

Preparation of Pt/C catalyst on Ni foam. To prepare the Pt/C electrode for comparison, 40 mg of Pt/C and 60 μL of Nafion were dispersed in 540 μL of ethanol and 400 μL of DI water, and the mixture was ultrasonicated for 30 min. The dispersion was then coated onto a Ni foam substrate, which was dried in air overnight.

Materials characterization. The morphology and nanostructure of the samples were determined using scanning electron microscopy (SEM, LEO 1525) and transmission electron microscopy (TEM, JEOL 2010F) coupled with energy dispersive X-ray (EDX) spectroscopy. The phase composition of the samples was characterized by X-ray diffraction (XRD) (PANalytical X'pert PRO diffractometer with a Cu K α radiation source). X-ray photoelectron spectroscopy (XPS) (PHI Quantera XPS) was performed using a PHI Quantera SXM Scanning X-ray Microprobe.

Electrochemical tests. The electrochemical performance of the catalysts was tested at room temperature on an electrochemical station (Gamry, Reference 600) in a standard three-electrode system in 1 M KOH electrolyte with the prepared sample used as the working electrode, a graphite rod used as the counter electrode, and a standard Hg/HgO electrode used as the reference. Cyclic voltammetry (CV) sweeps between 0.02 V and -0.25 V vs. reversible hydrogen electrode (RHE) at a scan rate of 50 mV s^{-1} were applied to electrochemically activate the catalysts prior to the HER tests. The HER polarization curves were performed with a sweep rate of 2 mV s^{-1} . Stability tests were carried out under constant overpotentials. Electrochemical impedance spectra (EIS) were measured at an overpotential of 150 mV from 0.1 Hz to 100 KHz with an amplitude of 10 mV. All of the measured potentials vs. the Hg/HgO were converted to RHE by the Nernst equation ($E_{\text{RHE}} = E_{\text{Hg/HgO}} + 0.0591 \text{ pH} + 0.098$). All of the curves were reported with iR compensation (85%).

2. Supplementary Figures

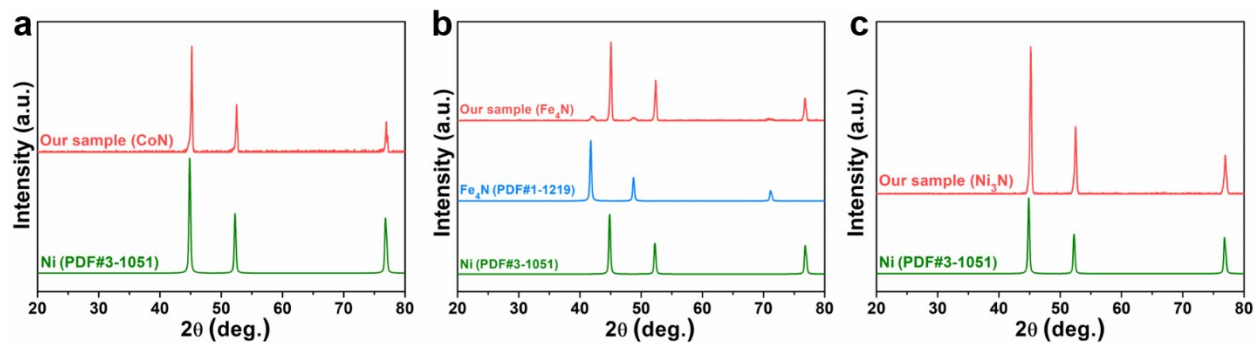


Fig. S1 XRD patterns of the as-prepared (a) CoN, (b) Fe_4N , and (c) Ni_3N on Ni foam.

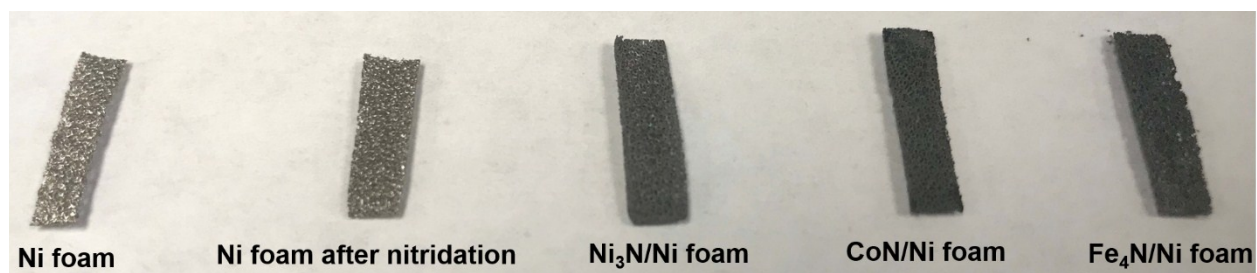


Fig. S2 Optical images of as-prepared samples on the Ni foam.

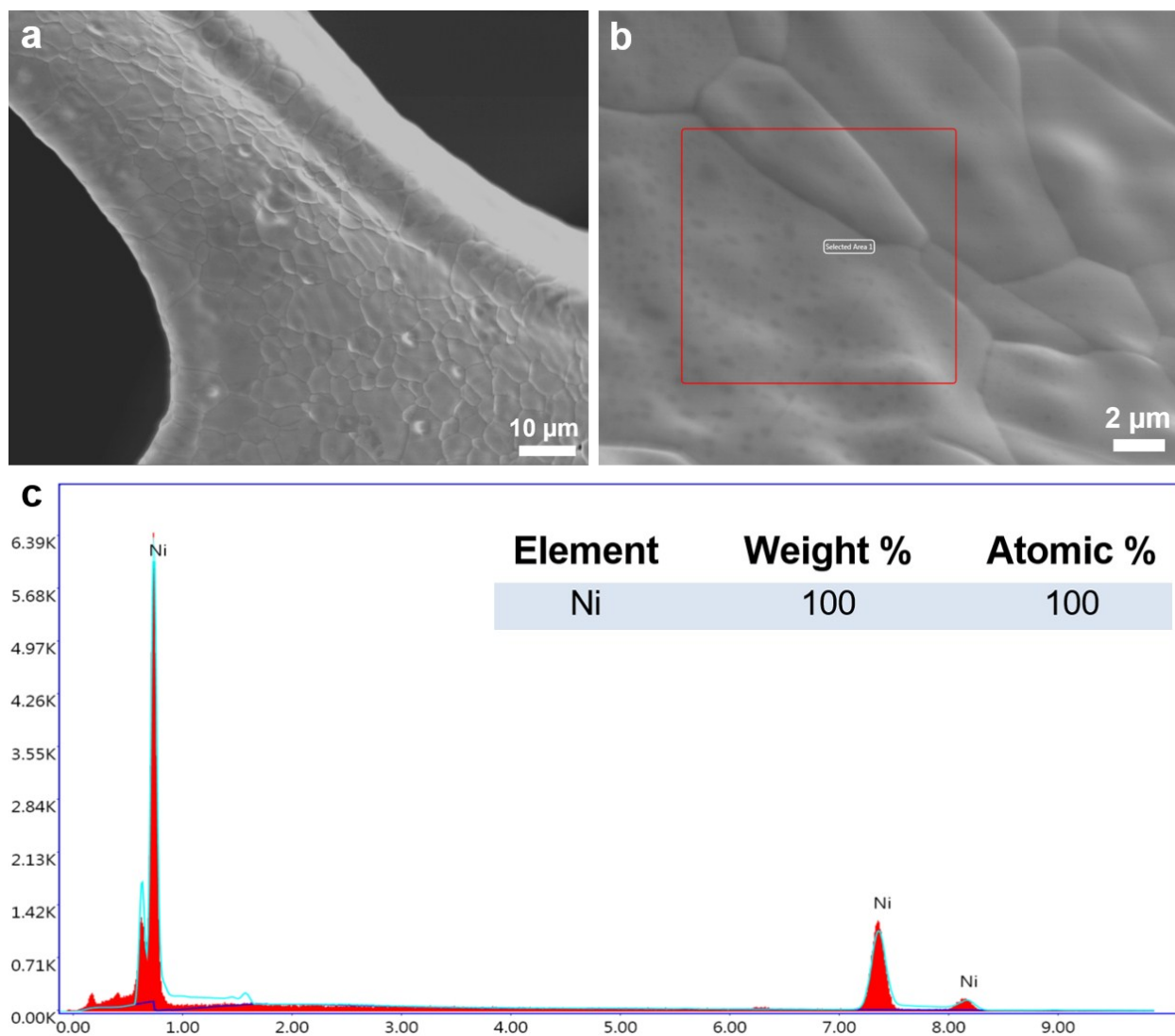


Fig. S3 (a, b) SEM images at different magnifications, and (c) SEM energy dispersive X-ray (EDX) spectrum in the selected area in (b) of the sample derived from direct nitridation of Ni foam.

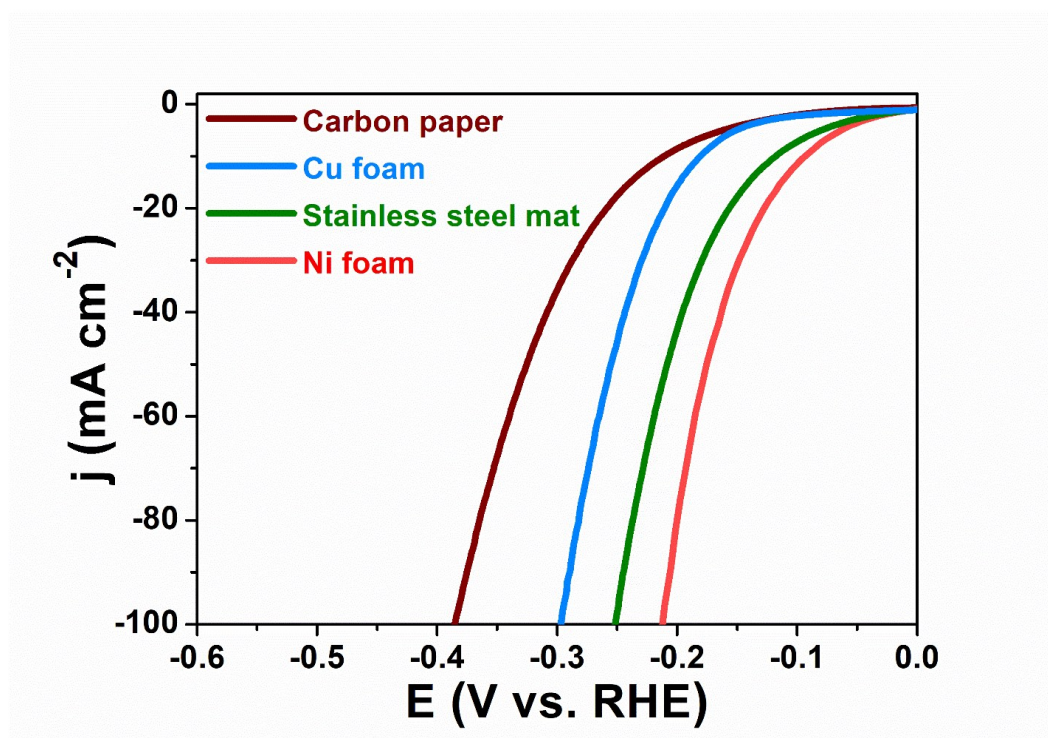


Fig. S4 HER polarization curves (1 M KOH) of CoN grown on different substrates.

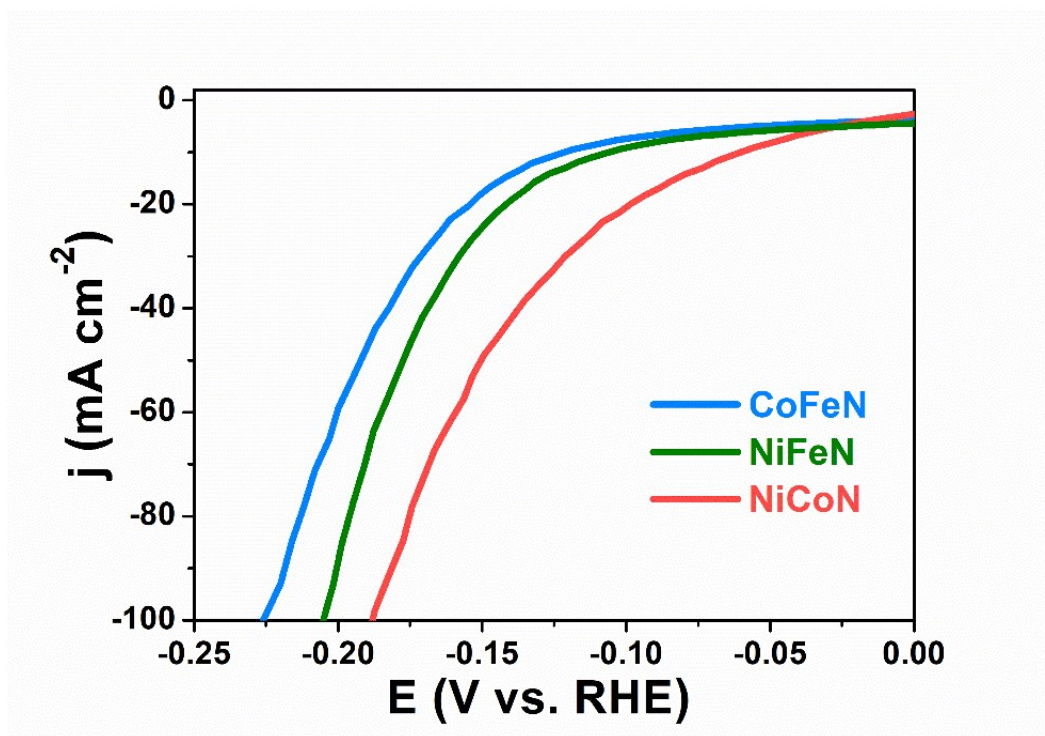


Fig. S5 HER polarization curves of bimetallic nitrides of CoFeN, NiFeN, and NiCoN grown on Ni foam in 1 M KOH.

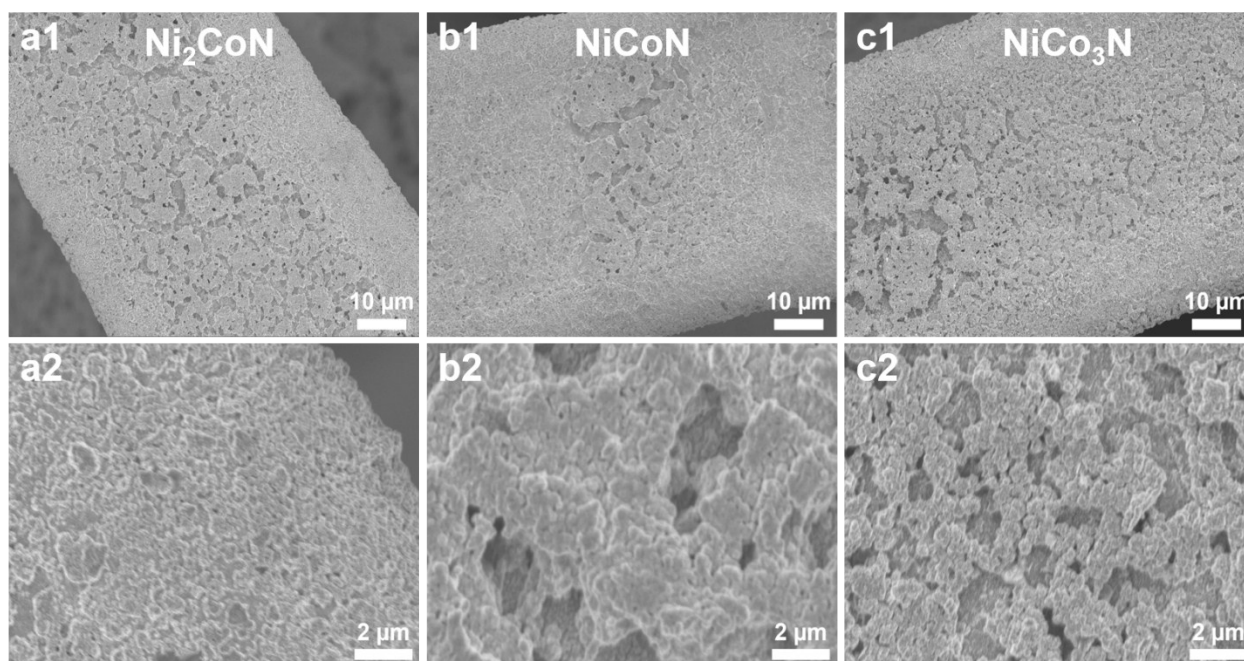


Fig. S6 SEM images at different magnifications of Ni-doped CoN samples prepared with different respective concentrations of precursor inks. (a1 and a2) Ni_2CoN , (b1 and b2) NiCoN , and (c1 and c2) NiCo_3N .

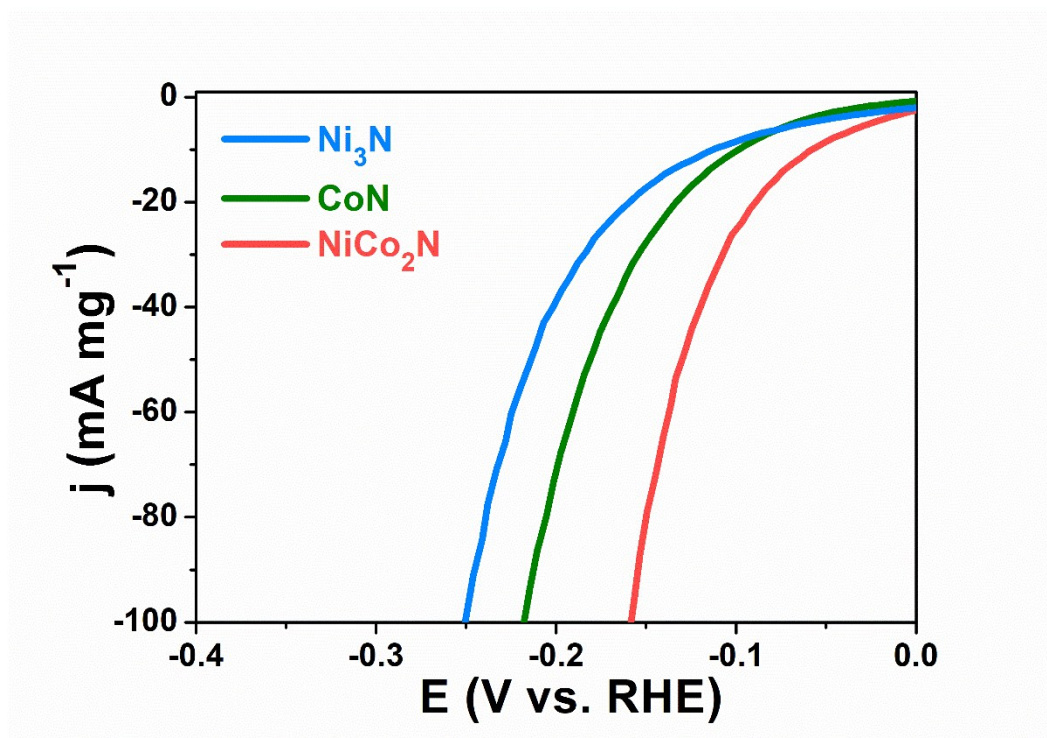


Fig. S7 HER polarization curves of different catalysts normalized by the loading mass to evaluate the mass activity. The loading mass of CoN, Ni₃N, and NiCo₂N is around 1.12, 0.83, and 1.29 mg cm⁻², respectively.

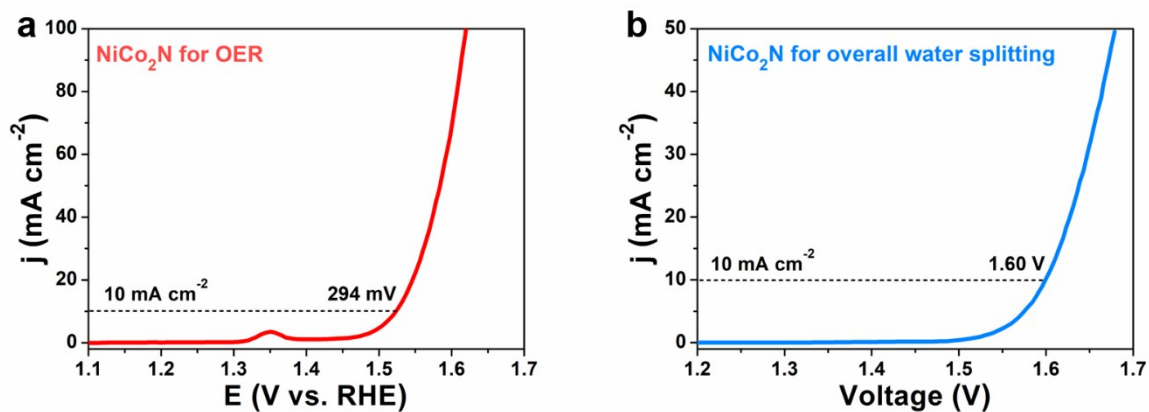


Fig. S8 (a) OER polarization curve of NiCo₂N, and (b) overall water splitting performance of NiCo₂N using it as both anode and cathode. All tests were conducted in 1 M KOH at room temperature.

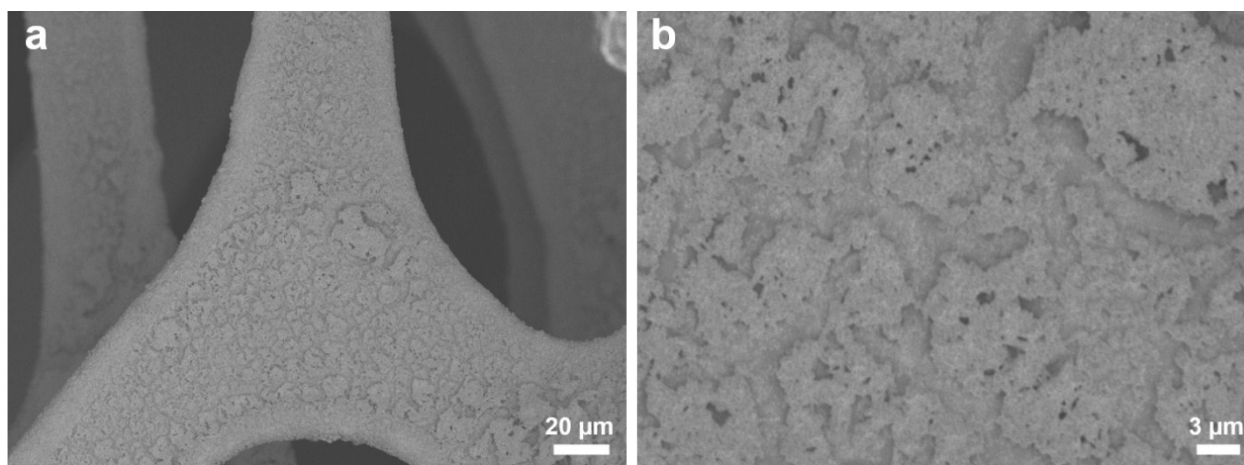


Fig. S9 SEM images of the NiCo₂N catalyst after long-term HER stability test.

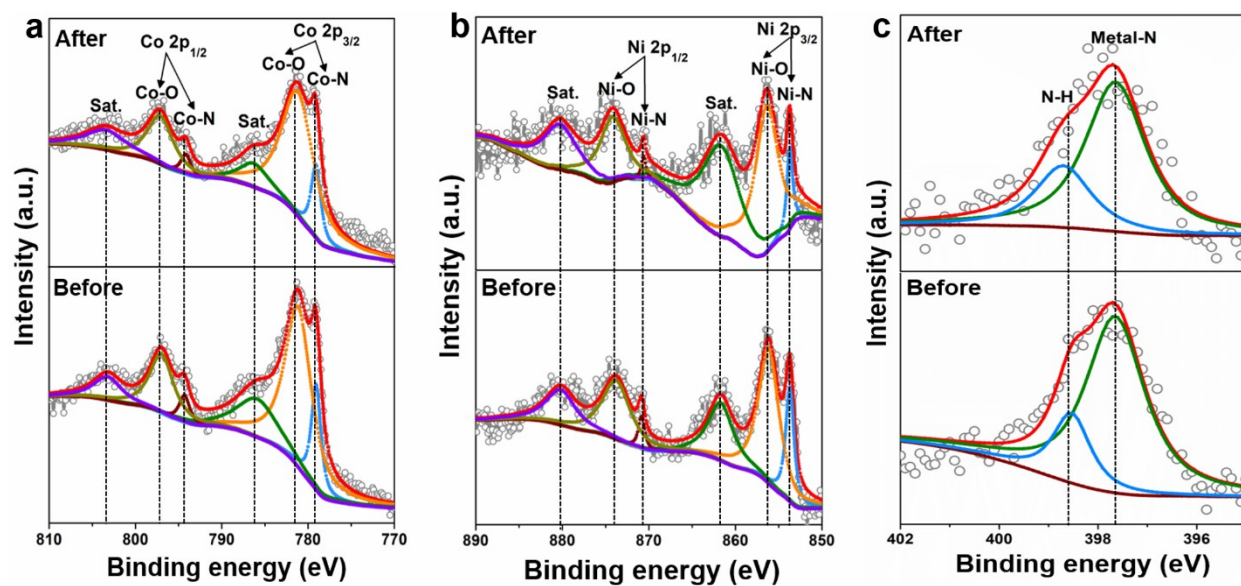


Fig. S10 High-resolution XPS spectra of (a) Co 2p, (b) Ni 2p, and (c) N 1s for the NiCo₂N catalyst before and after the stability test.

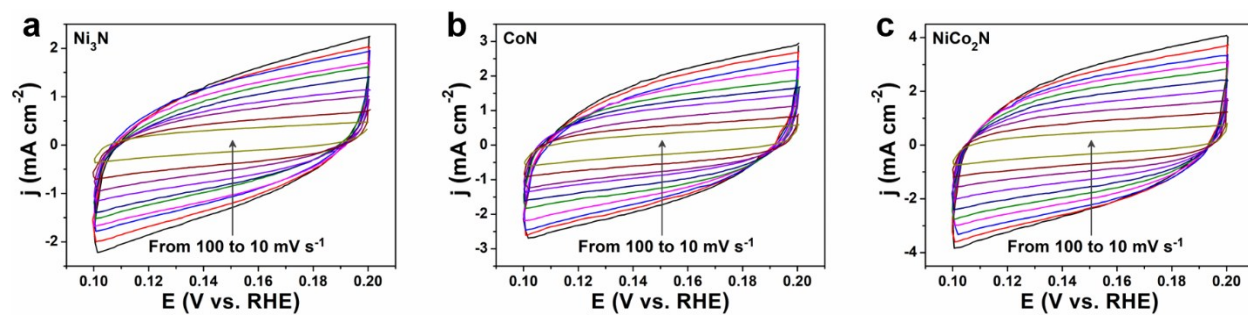


Fig. S11 Cyclic voltammograms of (a) Ni_3N , (b) CoN , and (c) NiCo_2N at scan rates ranging from 10 mV s^{-1} to 100 mV s^{-1} with an interval point of 10 mV s^{-1} .

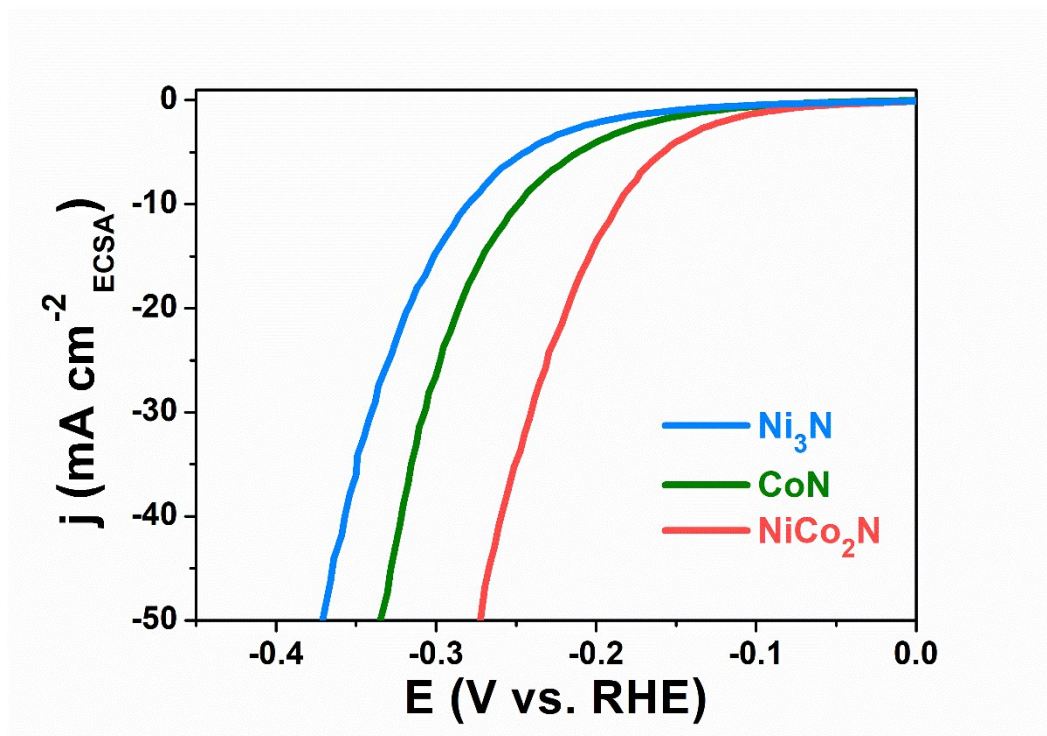


Fig. S12 HER polarization curves of different catalysts normalized by the ECSA.

3. Turnover frequency calculations

To calculate the per-site turnover frequency (TOF), we used the following formula according to previous reports:^{1, 2}

$$TOF \text{ per site} = \frac{\# \text{ Total Hydrogen Turn Overs/cm}^2 \text{ geometric area}}{\# \text{ Surface Sites /cm}^2 \text{ geometric area}}$$

The number of total hydrogen turn overs was calculated from the current density using the following equation:

$$\begin{aligned} \#_{H_2} &= \left(j \frac{mA}{cm^2} \right) \left(\frac{1 C s^{-1}}{1000 mA} \right) \left(\frac{1 mol e^{-}}{96485.3 C} \right) \left(\frac{1 mol H_2}{2 mol e^{-}} \right) \left(\frac{6.022 \times 10^{23} H_2 \text{ molecules}}{1 mol H_2} \right) \\ &= \frac{H_2/s}{cm^2} \text{ per } \frac{mA}{cm^2} \end{aligned}$$

The upper limit of the number of active sites was calculated based on the hypothesis that all Co and Ni atoms in the CoN, Ni₃N, and NiCo₂N catalysts form active centers and that all of them are accessible to the electrolyte. The real number of active sites should be considerably lower than the calculated value. The loading mass values of CoN, Ni₃N, and NiCo₂N are around 1.12, 0.83, and 1.29 mg cm⁻², respectively. The active site density values are:

$$\text{CoN: } \frac{1.12}{1000} \times \frac{1}{72.94} \times 6.022 \times 10^{23} \text{ sites/cm}^2 = 9.25 \times 10^{18} \text{ sites/cm}^2$$

$$\text{Ni}_3\text{N: } \frac{0.83}{1000} \times \frac{1}{190.08} \times 6.022 \times 10^{23} \times 3 \text{ sites/cm}^2 = 7.92 \times 10^{18} \text{ sites/cm}^2$$

$$\text{NiCo}_2\text{N: } \frac{1.29}{1000} \times \frac{1}{190.56} \times 6.022 \times 10^{23} \times 3 \text{ sites/cm}^2 = 1.22 \times 10^{19} \text{ sites/cm}^2$$

Therefore, the per-site TOF values for the different catalysts are calculated as follows:

$$\text{CoN:} \left(\frac{3.12 \times 10^{15} \frac{H_2/s}{cm^2}}{\frac{mA}{cm^2}} \right) \left(j \frac{mA}{cm^2} \right) \left(\frac{1 cm^2}{9.25 \times 10^{18} \text{ surface sites}} \right) = 0.00034 j \frac{H_2/s}{\text{surface site}}$$

$$\text{Ni}_3\text{N:} \left(\frac{3.12 \times 10^{15} \frac{H_2/s}{cm^2}}{\frac{mA}{cm^2}} \right) \left(j \frac{mA}{cm^2} \right) \left(\frac{1 cm^2}{7.92 \times 10^{18} \text{ surface sites}} \right) = 0.00039 j \frac{H_2/s}{\text{surface site}}$$

$$\text{NiCo}_2\text{N:} \left(\frac{3.12 \times 10^{15} \frac{H_2/s}{cm^2}}{\frac{mA}{cm^2}} \right) \left(j \frac{mA}{cm^2} \right) \left(\frac{1 cm^2}{1.22 \times 10^{19} \text{ surface sites}} \right) = 0.00026 \frac{H_2/s}{\text{surface site}}$$

4. References

- (1). H.-W. Liang, S. Brüller, R. Dong, J. Zhang, X. Feng and K. Müllen, *Nat. Commun.*, 2015, **6**, 7992.
- (2). Z. Zhao, F. Qin, S. Kasiraju, L. Xie, M. K. Alam, S. Chen, D. Wang, Z. Ren, Z. Wang and L. C. Grabow, *ACS Catal.*, 2017, **7**, 7312-7318.